Magnetic structure of thin films of Fe_xMn_{1-x} on Cu(100)/Co by the fully relativistic screened KKR method

L. Szunyogh
Center for Computational Materials Science, Technische Universität Wien, Getreidemarkt 9/134, 1060 Vienna, Austria and Department of Theoretical Physics, Budapest University of Technology and Economics, Budafoki út. 8, Budapest 1521, Hungary

J. Zabloudil
Center for Computational Materials Science, Technical University of Vienna, Getreidemarkt 9/134, Vienna A-1060, Austria

P. Weinberger
Center for Computational Materials Science, Technical University of Vienna, Getreidemarkt 9/134, Vienna A-1060, Austria

F. Offi
Max-Planck-Institut für Mikrostrukturphysik, Weinberg 2, Halle/Saale D-06120, Germany

W. Kuch
Max-Planck-Institut für Mikrostrukturphysik, Weinberg 2, Halle/Saale D-06120, Germany

J. Kirschner
Max-Planck-Institut für Mikrostrukturphysik, Weinberg 2, Halle/Saale D-06120, Germany
(Received 8 August 2002; published 28 February 2003)

The fully relativistic screened Korringa-Kohn-Rostoker method is used to discuss the electronic structure and magnetic properties of Fe_xMn_{1-x} overlayers on Cu(100)/Co. It is found that in this system, energetically low-lying antiferromagnetic configurations most likely are the cause for the experimentally observed antiferromagnetism. In all cases investigated, the ground state corresponds to the (in-plane) ferromagnetic configuration; the Fe_xMn_{1-x} overlayers do carry a small (concentration averaged) magnetic moment. In very good agreement with experiment, two overlayer thicknesses, namely, at 3 and 10 ML, are traced, at which either this moment nearly vanishes (3 ML) or different types of antiferromagnetic configurations apply (10 ML).

DOI: 10.1103/PhysRevB.67.054418 PACS number(s): 75.30.Gw, 75.70.Ak, 75.70.Cn

I. INTRODUCTION

Antiferromagnetic/ferromagnetic heterostructures turned out in the past to be of considerable interest because of possible applications in spin valve systems. Since in the bulk phase, fcc $Fe_{50}Mn_{50}$ is antiferromagnetic and of nearly the same lattice spacing as fcc Cu, with a rather small misfit as far as the interlayer distance is concerned, for Co overlayers on Cu(100), a combination of these three ingredients (Cu, Co, and $Fe_{50}Mn_{50}$) in one system seems to be ideally suited for the search of new properties. As usual, once these partial systems are combined in a multilayer system, virtually none of the characteristic bulk features seems to apply. Recent experimental investigations[1–4] of the system $Cu(100)/Co/Fe_{50}Mn_{50}$ revealed rather puzzling results: on the one hand typical features of antiferromagnetism, such as critical temperatures at which antiferromagnetism disappears, were found. At 10 ML $Fe_{50}Mn_{50}$ thickness, this critical temperature equals room temperature. On the other hand, ferromagnetic moments of Fe and Mn were also traced. It is therefore quite tempting to discuss these findings using an *ab initio* approach.

In the present paper, first the theoretical and computational details are briefly summarized, followed by a presentation of the results. In the following section, the main aspects of the experimental investigations are then reviewed and related to the theoretical results. The conclusion once again stresses the importance of the investigated system and the close relationship between theory and experiment.

II. THEORETICAL AND COMPUTATIONAL DETAILS

The fully relativistic spin-polarized screened Korringa-Kohn-Rostoker method for layered systems[5] is applied within the framework of the coherent-potential approximation[6] in order to calculate the electronic structure and magnetic properties of Fe_xMn_{1-x} overlayers on $Cu(100)/Co_6$. In all calculations, an fcc parent lattice[7] is assumed with a lattice spacing a_0 of 6.8309 a.u. (bulk fcc Cu), i.e., no layer relaxation is considered, and six Cu layers serve as buffer to the semi-infinite Cu substrate. In order to determine self-consistently within the local-density approximation[8] the effective potentials and effective exchange fields, a minimum of 45 $\mathbf{k}_\parallel$ points in the irreducible wedge of the surface brillouin zone (ISBZ) is used. All self-consistent calculations refer to a ferromagnetic (parallel) configuration $\mathcal{C}_0$ with the orientation of the magnetization pointing along the surface normal. In the present study, only collinear magnetic configurations are considered.

Let $\Delta E(\mathcal{C}_i)$ denote[5] the energy difference of a particular magnetic configuration $\mathcal{C}_i$ with respect to the reference configuration $\mathcal{C}_0$,

$$\Delta E(\mathcal{C}_i) = E(\mathcal{C}_i) - E(\mathcal{C}_0), \tag{1}$$

where $E(\mathcal{C}_i)$ and $E(\mathcal{C}_0)$ refer to grand potentials at $T=0$. If c_α^p denotes the respective concentrations of the constituents A and B in layer p, then in terms of the (inhomogeneous) CPA for layered systems,[6] $\Delta E(\mathcal{C}_i)$ is given by

$$\Delta E(\mathcal{C}_i) = \sum_{p=1}^{N} \Delta E^p(\mathcal{C}_i) = \sum_{p=1}^{N} \sum_{\alpha=A,B} c_\alpha^p \Delta E_\alpha^p(\mathcal{C}_i), \tag{2}$$

$$E_\alpha^p(\mathcal{C}_i) = \int_{\epsilon_b}^{\epsilon_F} n_\alpha^p(\epsilon;\mathcal{C}_i)(\epsilon - \epsilon_F) d\epsilon, \tag{3}$$

where N is the total number of layers considered, the $n_\alpha^p(\epsilon;\mathcal{C}_i)$ are component and layer projected density of states corresponding to the magnetic configuration $\mathcal{C}_i$, ϵ_b denotes the bottom of the valence band, and ϵ_F is the Fermi energy of the (nonmagnetic) substrate.

If in a similar manner for a particular magnetic configuration $\mathcal{C}_i$ $m_\alpha^p(\mathcal{C}_i)$ denotes the magnetic moment of constituent α in layer p, then the layer-resolved concentration-averaged moments are given by[5]

$$\langle m^p(\mathcal{C}_i)\rangle = \sum_{\alpha=A,B} c_\alpha^p m_\alpha^p(\mathcal{C}_i). \tag{4}$$

Furthermore, since experimentally layer-resolved magnetic moments cannot be recorded, it is perhaps useful to define layer- and concentration-averaged moments as follows:

$$\langle M(\mathcal{C}_i)\rangle = \frac{1}{n} \sum_{p=1}^{n} \langle m^p(\mathcal{C}_i)\rangle, \tag{5}$$

where n is restricted to the number of Fe_xMn_{1-x} overlayers, since—as will be shown—by including also the Co layers, simply an averaged moment per Co layer of about $1.654\mu_B$ has to be added, provided that the orientation of the magnetization in at least the first Fe_xMn_{1-x} layer is oriented parallel to the Co slab.

If in Eq. (1) $\mathcal{C}_i$ refers to a magnetic configuration in which the orientation of the magnetization in all layers is uniformly perpendicular to $\mathcal{C}_0$, then $\Delta E(\mathcal{C}_i)$ usually is called the band energy part of the magnetic anisotropy energy.[5] According to the definition given in Eq. (1), this implies that

$$\Delta E(\mathcal{C}_i) = \begin{cases} >0, & \mathcal{C}_0 \text{ preferred configuration} \\ <0, & \mathcal{C}_i \text{ preferred configuration.} \end{cases} \tag{6}$$

All energy differences in Eq. (1) are evaluated (at zero temperature) in terms of the magnetic force theorem via an integration in the upper half of the complex energy plane along a contour that starts at a real energy well below the valence band and ends at the Fermi energy. For these calculations, a total of 990 $\mathbf{k}_\parallel$ points in the ISBZ is used, which—as was shown[5] in the case of magnetic anisotropy energies—guarantees well-converged results.

It should be noted that although layer relaxation is very important for the structural properties of the investigated films, it is of much less importance once energy differences between two magnetic configurations, see Eq. (1), are taken. One can assume quite safely that for a given sequence of layers the structural energies due to layer relaxation for two different magnetic configurations are rather similar in value, and therefore cancel out in the energy difference between these two magnetic configurations.

Since in the following presentation of the results quite a few different magnetic configurations are discussed, these configurations will in general be denoted by Co:$[u]$/(FeMn):$i[u]j[d]k[p]$, meaning that for a total of $n=i+j+k$ overlayers of (Fe_xMn_{1-x}) on $Cu(100)/Co_6$, the orientation of the magnetization in the first i (Fe_xMn_{1-x}) layers is aligned parallel to the one in the Co slab, in the subsequent j layers antiparallel, followed by k layers oriented perpendicularly. The reference configuration in this terminology is then simply given by Co:$[u]$/(FeMn):$n[u]$, meaning that in all layers the orientation of the magnetization is parallel to the surface normal.

In most cases the concentration x is simply 0.5; however, in a few cases also homogeneous alloys of different concentrations are considered. Since it cannot be ruled out that segregation (interdiffusion) phenomena occur, this is taken into account by inhomogeneous alloying such that

$$\frac{1}{n} \sum_{p=1}^{n} x_\alpha^p = \frac{1}{2}, \tag{7}$$

with α=Fe, Mn, and n being the number of Fe_xMn_{1-x} overlayers.

III. RESULTS

A. Antiparallel magnetic configurations

In Fig. 1, various energy differences $\Delta E(\mathcal{C}_i)$ [see Eq. (1)] for $Cu(100)/Co_6/(Fe_{0.5}Mn_{0.5})_n$, $n=3,4$, are shown. As can be seen from this figure by considering only collinear magnetic configurations (parallel or antiparallel configurations), the energetically lowest antiparallel configuration is quite a bit higher for $n=3$ than for $n=4$. Some of the configurations shown in Fig. 1 are considerably higher in energy than the parallel (ferromagnetic) ground-state configuration. It should be noted that in this figure only the magnetic configuration in the $Fe_{0.5}Mn_{0.5}$ film is marked explicitly, the orientation of all layers in the Co slab is simply $[u]$.

In Fig. 2, the energetically lowest antiparallel configurations are displayed versus the number of $Fe_{0.5}Mn_{0.5}$ overlayers. It is evident that there are two special cases, namely, for $n=3$ and for $n=10$, in all other cases $\Delta E(\mathcal{C}_i)$ varies only moderately around 6–7 [meV]. There seems to be a regime of Co:$[u]$/(FeMn):$(n-2)[u]2[d]$ configurations for $n<6$, followed by a regime of Co:$[u]$/(FeMn):$(n-4)[u]4[d]$ configurations for $6\leqslant n\leqslant 9$. Beyond $n=10$, the first half of $Fe_{0.5}Mn_{0.5}$ overlayers is aligned parallel to the Co slab, the second half being antiparallel. Clearly enough, as n in-

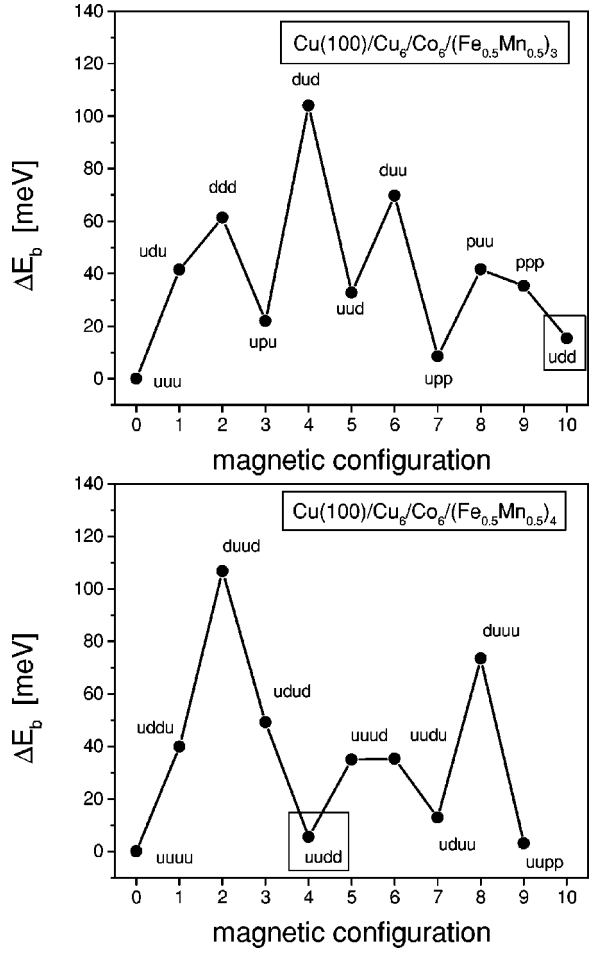

FIG. 1. $\Delta E(\mathcal{C}_i)$ for $Cu(100)/Cu_6/Co_6/(Fe_{0.5}Mn_{0.5})_n/Vac$, $n=3$ (top) and 4 (bottom). The symbols *u*, *d*, and *p*, correspond to parallel, antiparallel, and perpendicular aligments of the magnetization in a particular (FeMn) layer with the one in the Co slab. The lowest antiparallel magnetic configuration is marked by a box.

creases, the number of antiferromagnetic configurations increases dramatically. Fortunately, it turned out that for a given *n*, there are only a few energy regimes into which most of the $\Delta E(\mathcal{C}_i)$ fall. The energetically lowest $\Delta E(\mathcal{C}_i)$ can therefore be traced by a simple trial and error procedure. This approach was also used for $n=10$.

How close in energy, for a given number of $Fe_{0.5}Mn_{0.5}$ overlayers, some of these antiparallel configurations are can be seen from Fig. 3 in which in configurations of the type $Co:[u]/(FeMn):(n-m)[u]m[d]$ the number of antiparallel $(Fe_{0.5}Mn_{0.5})$, *m*, is varied. Taking, for example, the case of twelve overlayers, $\Delta E(\mathcal{C}_i)$ is almost constant for $2 \leqslant m \leqslant 11$. This particular feature seems to apply to all *n*, but $n=3,10$. However, while for $n=10$ a completely different curve is obtained, for $n=3$ the corresponding curve seems to be only slightly out of scale as far as the entry for $m=2$ is concerned. Figure 3 indicates that at a first glance, these two special cases are qualitatively different. It should be noted that in this figure only a characteristic selection of different values of *n* is shown.

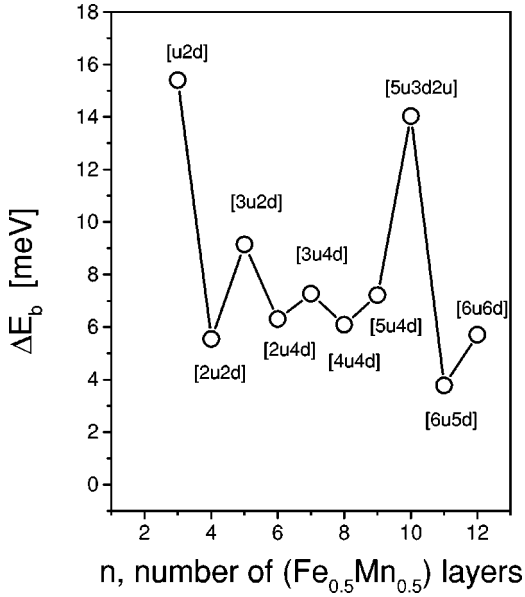

FIG. 2. $\Delta E(\mathcal{C}_i)$ corresponding to the lowest antiparallel magnetic configuration in $Cu(100)/Cu_6/Co_6/(Fe_{0.5}Mn_{0.5})_n/Vac$ versus *n*, the number of $(Fe_{0.5}Mn_{0.5})$ layers. The respective magnetic configurations in the (FeMn) films are marked explicitly.

In order to pinpoint the peculiarities for $n=3,10$ in Figs. 4–7, layerwise energy differences $\Delta E^p(\mathcal{C}_i)$, see Eq. (2), are displayed. In Fig. 4, the two energetically lowest antiparallel configurations for $n=3$ are compared to each other, see also

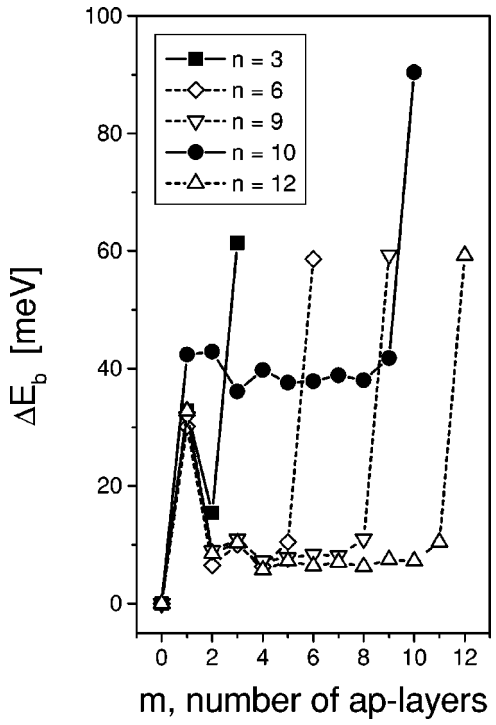

FIG. 3. $\Delta E(\mathcal{C}_i)$ corresponding to the magnetic configuration $Co:[u]/(FeMn):(n-m)[u]m[d]$ in $Cu(100)/Cu_6/Co_6/(Fe_{0.5}Mn_{0.5})_n/Vac$ versus *m*, the number of antiparallel $(Fe_{0.5}Mn_{0.5})$ layers counted from the right, see text. The total number of $Fe_{0.5}Mn_{0.5}$ layers, *n*, is marked explicitly.

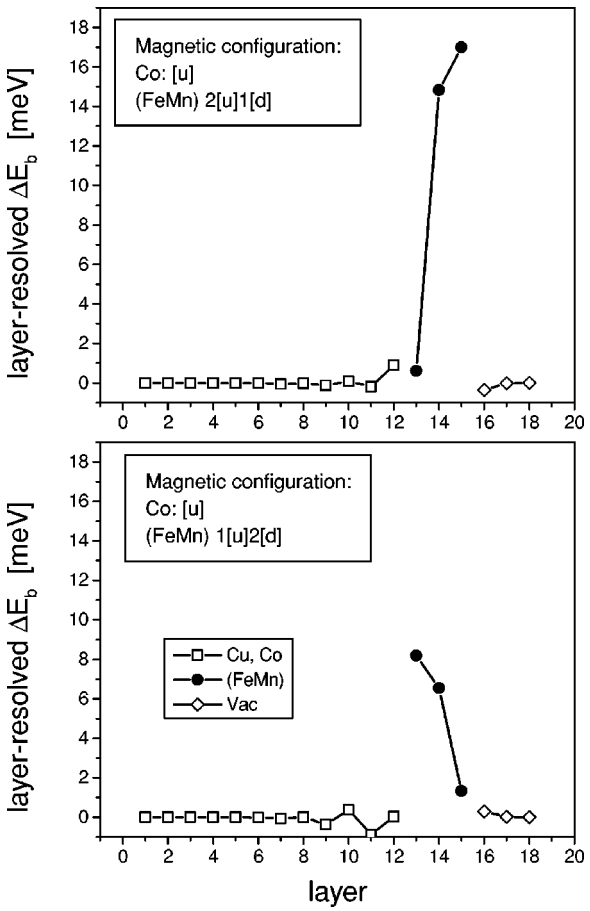

FIG. 4. Layer-resolved $\Delta E(\mathcal{C}_i)$ for $\mathrm{Cu}(100)/\mathrm{Cu}_6/\mathrm{Co}_6/(\mathrm{Fe}_{0.5}\mathrm{Mn}_{0.5})_n/\mathrm{Vac}$, $n=3$. The magnetic configuration is marked explicitly, and so are the various contributions to $\Delta E(\mathcal{C}_i)$.

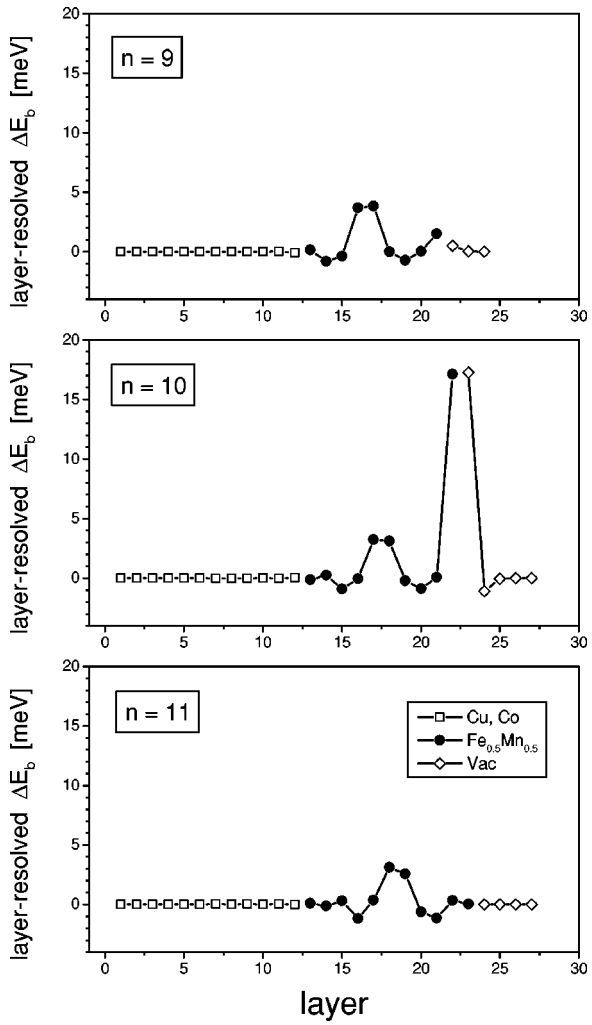

FIG. 5. Layer-resolved $\Delta E(\mathcal{C}_i)$ for $\mathrm{Cu}(100)/\mathrm{Cu}_6/\mathrm{Co}_6/(\mathrm{Fe}_{0.5}\mathrm{Mn}_{0.5})_n/\mathrm{Vac}$, $n=9,10,11$, corresponding to the magnetic configuration $\mathrm{Co}:[u]/(\mathrm{FeMn}):(n-5)[u]5[d]$. The various contributions to $\Delta E(\mathcal{C}_i)$ are marked explicitly.

Fig. 1. It can be seen that the main contributions to $\Delta E(\mathcal{C}_i)$ arise either from the two layers closest to the (FeMn)/Vac interface or from the two layers closest to the Co/(FeMn) interface. In Figs. 5 and 6, layerwise energy differences $\Delta E^p(\mathcal{C}_i)$ are displayed by keeping the configuration fixed and varying the number of $\mathrm{Fe}_{0.5}\mathrm{Mn}_{0.5}$ overlayers. In particular, these two figures show the reasons for the special kind of magnetic configurations, see Fig. 7, that apply for $n=10$: these are the contributions from the (FeMn)/Vac interface that have to be accommodated in the interior of the $\mathrm{Fe}_{0.5}\mathrm{Mn}_{0.5}$ film in order to minimize the antiparallel $\Delta E(\mathcal{C}_i)$.

All energy differences $\Delta E(\mathcal{C}_i)$ are in principle concentration dependent. This is shown in Fig. 8 for $\mathrm{Cu}(100)/\mathrm{Co}_6/(\mathrm{Fe}_x\mathrm{Mn}_{1-x})_4$ by varying the (homogeneous) concentration x. Only for $x \geqslant 0.5$, the magnetic configuration $\mathrm{Co}:[u]/(\mathrm{FeMn}):2[u]2[d]$ is the lowest in energy, for $x < 0.5$, the configuration with all $\mathrm{Fe}_x\mathrm{Mn}_{1-x}$ overlayers oriented antiparallel to the Co slab becomes almost as stable as the ferromagnetic (parallel) configuration. Since, in principle, segregation can also occur, in Fig. 9 (for the same overlayer thickness), the interdiffusion concentration x_d is varied such that the nominal concentration of Fe and Mn remains constant, see Eq. (7). As can be seen again, a different behavior of the $\Delta E(\mathcal{C}_i)$ is encountered: for Mn-enriched Co/(FeMn) interfaces, the magnetic configuration $\mathrm{Co}:[u]/(\mathrm{FeMn}):2[u]2[d]$ is not only stabilized, it even becomes the ground-state configuration. This already happens with an interdiffusion concentration x_d of about 0.45. If, however, Fe is enriched in this particular interface, then the configuration $\mathrm{Co}:[u]/(\mathrm{FeMn}):3[u]1[d]$ tends to become the ground state. For this to happen x_d has to assume values larger than 0.75.

The question then arises whether a (homogeneous) concentration dependence of the $\Delta E(\mathcal{C}_i)$ changes the peculiar feature discussed above for $n=10$. Figure 10 shows that this is not the case. In the vicinity of $x=0.5$ neither the curve shown in Fig. 3 is altered substantially with respect to x, nor do drastic changes occur for the antiparallel magnetic configurations lowest in energy. It should be noted that with the exception of the few cases shown in Figs. 8 and 9 at zero temperature, the ground state always refers to the ferromagnetic (parallel) configuration, although some of the differences to the energetically next higher antiparallel configuration can be very small indeed, namely, some may amount to

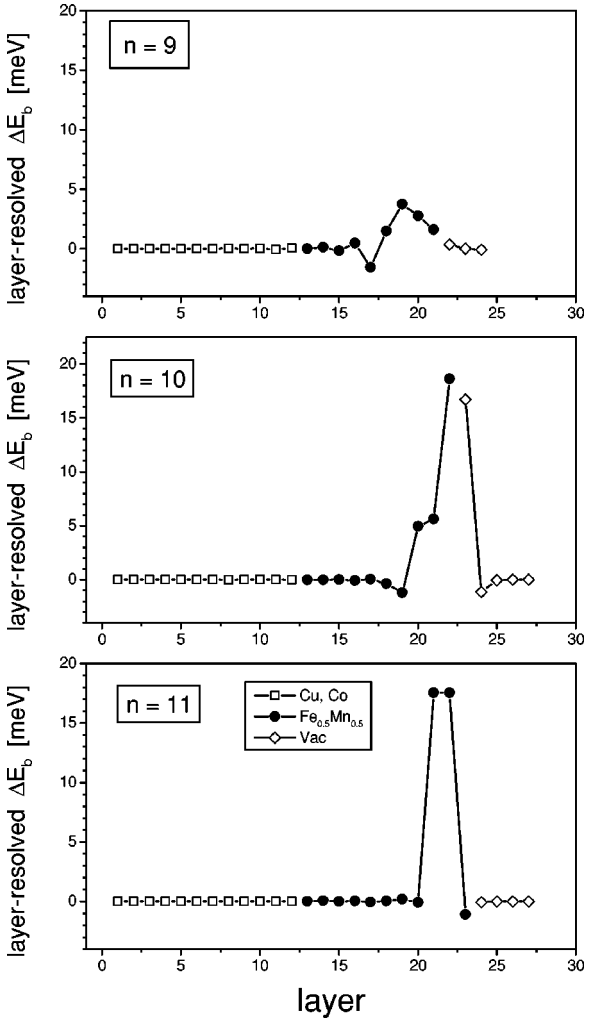

FIG. 6. Layer-resolved $\Delta E(\mathcal{C}_i)$ for $\mathrm{Cu}(100)/\mathrm{Cu}_6/\mathrm{Co}_6/(\mathrm{Fe}_{0.5}\mathrm{Mn}_{0.5})_n/\mathrm{Vac}$, $n=9,10,11$, corresponding to the magnetic configuration $\mathrm{Co}:[u]/(\mathrm{FeMn}):(n-2)[u]2[d]$. The various contributions to $\Delta E(\mathcal{C}_i)$ are marked explicitly.

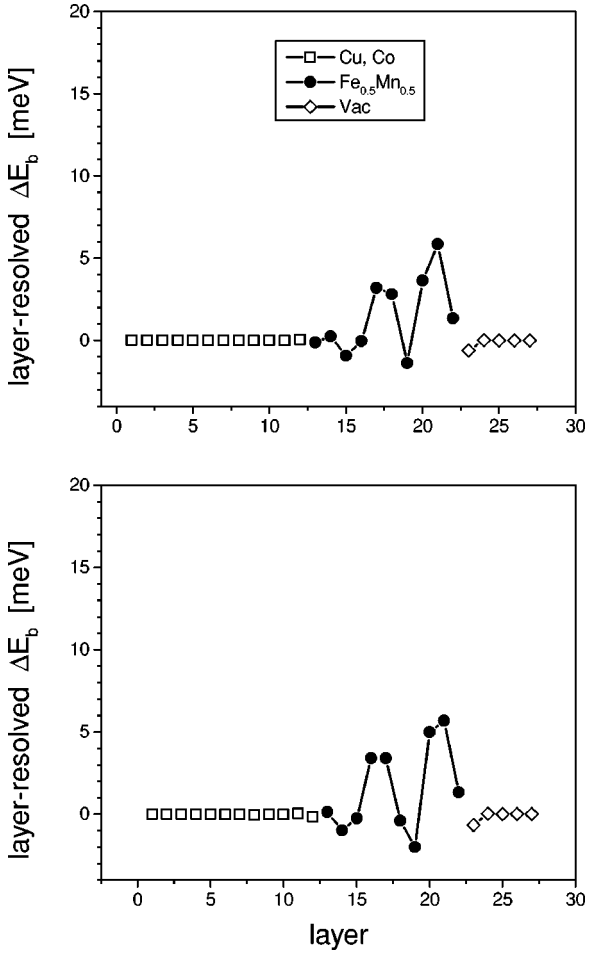

FIG. 7. Layer-resolved $\Delta E(\mathcal{C}_i)$ for $\mathrm{Cu}(100)/\mathrm{Cu}_6/\mathrm{Co}_6/(\mathrm{Fe}_{0.5}\mathrm{Mn}_{0.5})_{10}/\mathrm{Vac}$ corresponding to the magnetic configurations $\mathrm{Co}:[u]/(\mathrm{FeMn}):5[u]2[d]2[u]$ (top) and $\mathrm{Co}:[u]/(\mathrm{FeMn}):4[u]3[d]2[u]$ (bottom). The various contributions to $\Delta E(\mathcal{C}_i)$ are marked explicitly.

only a few meV, i.e., they are of the order of magnetic (surface) anisotropies.

B. Magnetic moments

In Figs. 11 and 12 the magnetic moments for $n=3,4$ are displayed in the parallel and a particular antiparallel magnetic configuration. As easily can be seen in this comparison, not only the componentlike magnetic moments in the $\mathrm{Fe}_{0.5}\mathrm{Mn}_{0.5}$ overlayer differ from each other substantially, but also do the averaged moments. Since in all layers respective Fe and Mn moments are aligned antiparallel to each other, the resulting layer-resolved averaged moment is rather small. From these figures it is evident that the contribution of the Co slab to the layer- and component-averaged magnetic moment $\langle M\rangle$, see also Eq. (5), is nearly independent from the configuration, provided that the orientation of the magnetization in at least the first $\mathrm{Fe}_{0.5}\mathrm{Mn}_{0.5}$ overlayer is parallel to the one in the Co slab. As already stated earlier, the contribution to $\langle M\rangle$ per Co layer would be about $1.654\mu_B$. Clearly enough, Figs. 11 and 12 can only serve as illustrations since for thicker $\mathrm{Fe}_{0.5}\mathrm{Mn}_{0.5}$ overlayers, the number of magnetic configurations for which magnetic moments ought to be shown simply increases drastically.

In Fig. 13, concentration averaged-moments, averaged over the number of $\mathrm{Fe}_{0.5}\mathrm{Mn}_{0.5}$ overlayers [see Eq. (5)], are compiled for the parallel and a particular antiparallel magnetic configuration, namely $\mathrm{Co}:[u]/(\mathrm{FeMn}):[u][d][u][d]\cdots$. As can be seen from Fig. 13 for $n\geqslant 4$ in the parallel configuration $\langle M\rangle$ becomes approximately constant, i.e., oscillates weakly around $0.3\mu_B$, and vanishes between 3 and 4 ML of $\mathrm{Fe}_{0.5}\mathrm{Mn}_{0.5}$. In the chosen antiparallel configuration, the moment also vanishes between 3 and 4 ML of $\mathrm{Fe}_{0.5}\mathrm{Mn}_{0.5}$ and oscillates around $-0.05\mu_B$ for larger values of n. From Fig. 13, it has to be concluded that at about $n=3$, the contributions to the layer-averaged moment from the overlayer vanishes, i.e., only the contributions from the Co slab remain.

C. Band energy part of the magnetic anisotropy energy

In Fig. 14, the band energy part of the magnetic anisotropy energy $\Delta E(\mathcal{C}_i)$ is displayed versus the number of

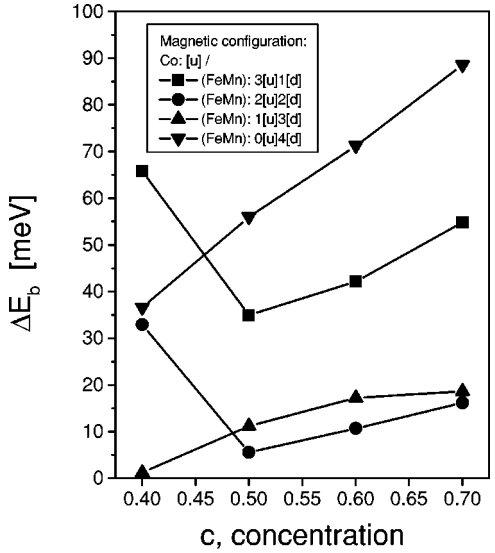

FIG. 8. Concentration dependent $\Delta E(\mathcal{C}_i)$ in Cu(100)/Cu_6/Co_6/$(Fe_xMn_{1-x})_4$/Vac. The various antiparallel magnetic configurations investigated are marked explicitly.

$Fe_{0.5}Mn_{0.5}$ overlayers. As can be seen, this quantity is rather small and oscillates around 0.015 meV with respect to the number of $Fe_{0.5}Mn_{0.5}$ overlayers. A layer-resolved representation for $n=12$, see Fig. 15, reveals that the main contributions to $\Delta E(\mathcal{C}_i)$ arise from the (FeMn)/Vac interface and from the Co slab. It should be noted that a positive value of $\Delta E(\mathcal{C}_i)$ indicates that a perpendicular orientation of the magnetization for a parallel magnetic configuration is preferred. However, since the band energy part of the magnetic anisotropy energy is rather very small, the magnetic dipole-dipole interaction (shape anisotropy) arising mostly from the Co slab dominates the magnetic anisotropy energy, i.e., puts the preferred orientation of the magnetization in plane.

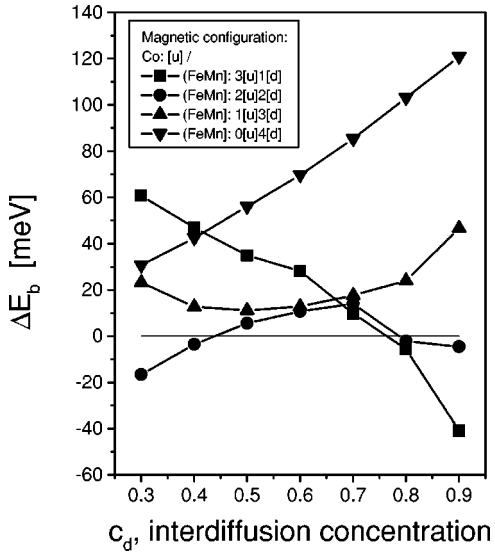

FIG. 9. $\Delta E(\mathcal{C}_i)$ in Cu(100)/Cu_6/Co_6/$(Fe_{x_d}Mn_{1-x_d})(Fe_{1-x_d}Mn_{x_d})(Fe_{1-x_d}Mn_{x_d})(Fe_{x_d}Mn_{1-x_d})$/Vac versus the interdiffusion concentration x_d. The various antiparallel magnetic configurations investigated are marked explicitly.

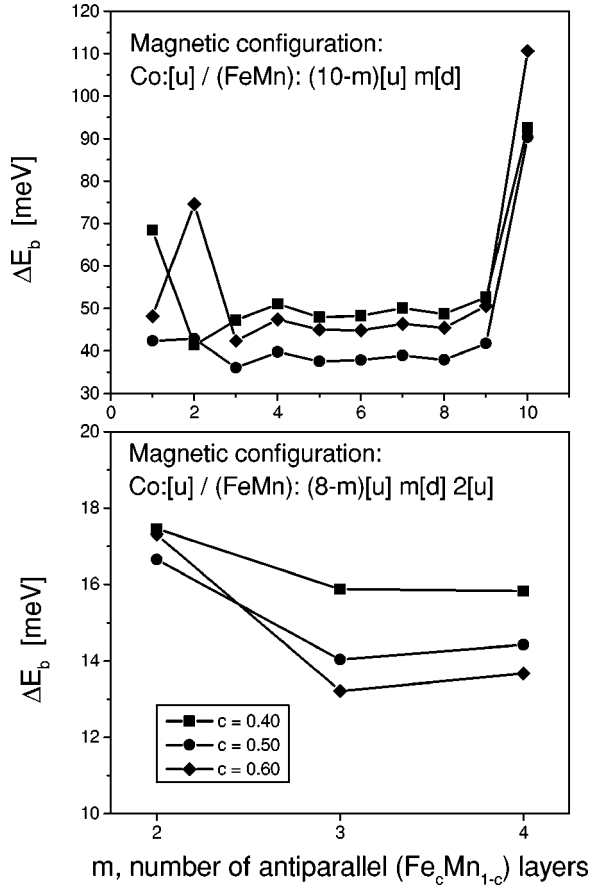

FIG. 10. Concentration-dependent $\Delta E(\mathcal{C}_i)$ in Cu(100)/Cu_6/Co_6/$(Fe_xMn_{1-x})_{10}$/Vac. The various antiparallel magnetic configurations investigated and the concentration x are marked explicitly.

IV. DISCUSSION AND COMPARISON TO EXPERIMENT

In Refs. 2 and 3, Offi *et al.* discussed the structural and magnetic properties of Fe_xMn_{1-x} thin films on Cu(001) and on Co_6/Cu(001) in terms of experimental investigations.[4] Quoting them in a compressed manner, they find as structural properties: (1) full evidence in terms of low-energy electron-diffraction measurements that $Fe_{50}Mn_{50}$ films keep the ''fcc'' structure when grown on Cu(001) and on Co/Cu(001), basically because the lattice mismatch between bulk $Fe_{50}Mn_{50}$ and bulk Cu is less than 1%, which seems to apply also to a Co/Cu(001) substrate; (2) the growth mode is pseudomorphic; (3) even in the initial stage of growth of $Fe_{50}Mn_{50}$ on Co/Cu(001), no superstructures are formed. As far as magnetic properties are concerned, they encountered rather surprising features in measuring hysteresis loops at room temperature in the longitudinal MOKE geometry: (1) the coercivity H_c is suddenly increased at about 10 ML of $Fe_{50}Mn_{50}$; (2) the remanence M_r shows a rather complicated behavior with respect to the overlayer thickness by having a round peak at about 2 ML of $Fe_{50}Mn_{50}$ and staying approximately constant for thicknesses between 4 and 9 ML; (3) the critical temperature at which antiferromagnetic ordering disappears increases above room temperature for thicknesses

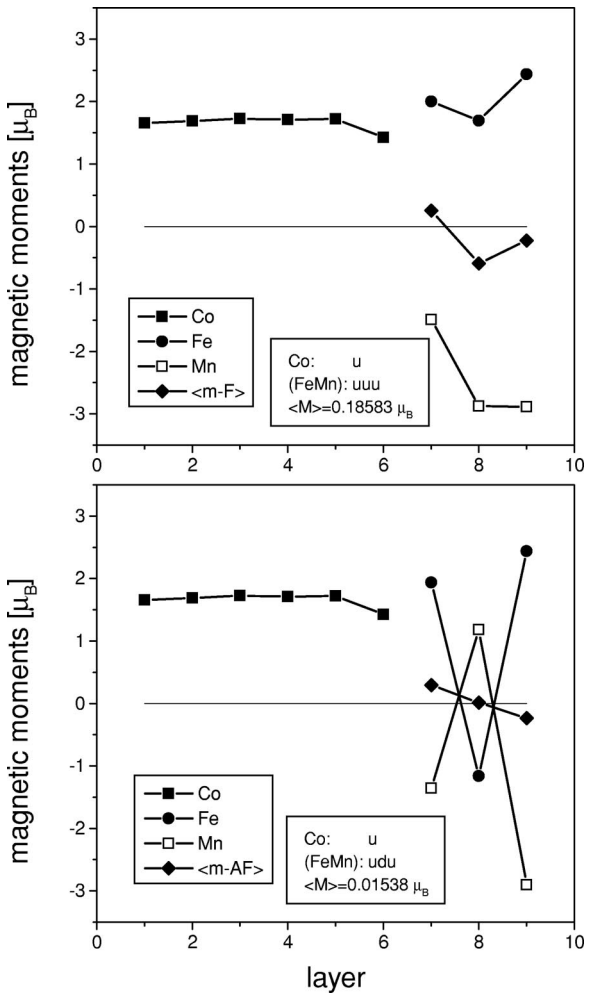

FIG. 11. Layer-resolved magnetic moments in Cu(100)/Cu_6/Co_6/$(Fe_{0.5}Mn_{0.5})_3$/Vac. The various constituents and the concentration-averaged moment are marked explicitly. The top part corresponds to the parallel magnetic configuration, the lower part to a particular antiparallel magnetic configuration.

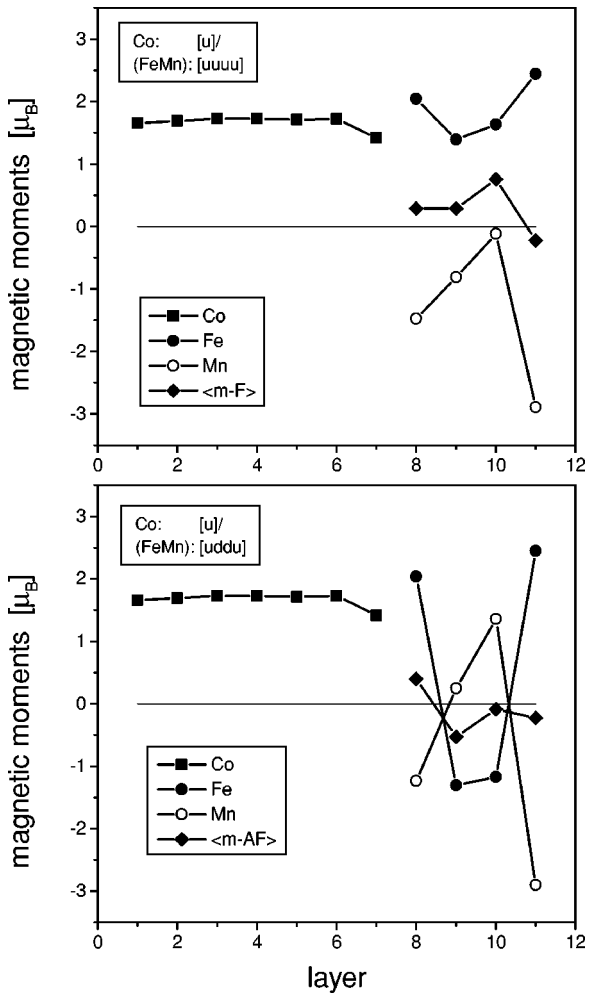

FIG. 12. Layer-resolved magnetic moments in Cu(100)/Cu_6/Co_6/$(Fe_{0.5}Mn_{0.5})_4$/Vac. The various constituents and the concentration-averaged moment are marked explicitly. The top part corresponds to the parallel magnetic configuration, the lower part to a particular antiparallel magnetic configuration.

beyond 9 ML, at 10 ML it corresponds to about room temperature; (4) this critical temperature seems to be concentration dependent since it is higher for Mn concentrations above 50%. In terms of photoemission electron microscopy, further, even more surprising facts were revealed: (1) beyond an overlayer thickness of 10 ML, suddenly different domain patterns evolved at room temperature; (2) the ''observed'' Fe moments seem to be coupled ferromagnetically to Co, while the direction of the observed Mn moments depends on the layer sequence; (3) the ferromagnetic signal does not change at the critical thicknesses for antiferromagnetic order at room temperature, namely, 10 ML; (3) below 3 ML of $Fe_{50}Mn_{50}$, the magnetic contrast in recorded Fe images is much stronger than in all other cases investigated. Summed up in a single sentence, their experiments provided ''*evidence that the contact with the Co film induces ferromagnetic moments in Fe and Mn*'' independent of the thickness of the overlayers.

It seems that whatever these authors collected in terms of experimental evidence is almost exactly reflected in the present theoretical investigations: (1) Figures 1–3 prove that in all cases investigated, the ground state in Cu(100)/Co_6/$(Fe_{0.5}Mn_{0.5})$ is a ferromagnetic one with an in-plane orientation of the magnetization, see the discussion with respect to Figs. 14 and 15; (2) Beyond 3 ML of $Fe_{0.5}Mn_{0.5}$, the layer- and concentration-averaged (ferromagnetic) moment, see Fig. 13, is indeed small and nearly independent of the overlayer thickness; (3) A thickness of 10 ML of $Fe_{0.5}Mn_{0.5}$ turns out to be a kind of singular thickness beyond which simpler antiparallel configurations seem to apply; (4) The observed critical temperature for antiferromagnetic ordering no longer is a big surprise, since all energetically low-lying antiparallel configurations correspond to energy differences of below 10 meV (with respect to the parallel reference configuration). Since 150 K correspond to about 14 meV, at room temperature all low-lying antiparallel magnetic configurations can be reached; (6) Even the rather broad hysteresis loops in the MOKE measurements do have some nondynamical origins. Viewing the applied field as a

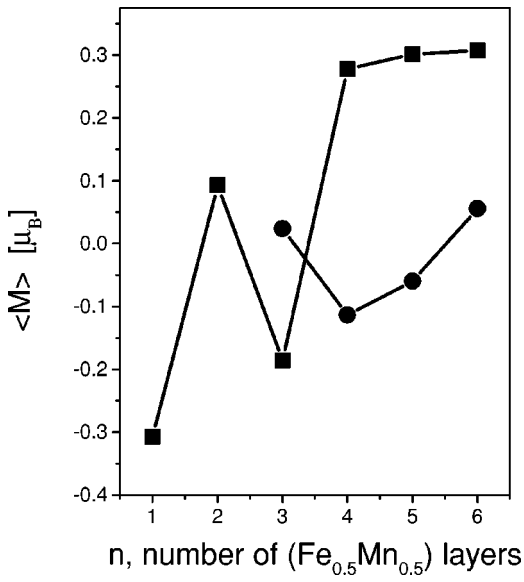

FIG. 13. Layer- and concentration-averaged magnetic moments $\langle M \rangle$, in $Cu(100)/Cu_6/Co_6/(Fe_{0.5}Mn_{0.5})_n/Vac$ versus n, the number of $(Fe_{0.5}Mn_{0.5})$ layers. Squares correspond to the parallel configuration $Co:[u]/(FeMn):n[u]$, circles to the configuration $Co:[u]/(FeMn):[u][d][u][d]\cdots$.

continuous energy by increasing (or decreasing) this energy, quite a few antiparallel magnetic configurations of comparable energy have to be formed until switching is observed. However, it needs to be evaluated theoretically[9–11] which parts of this system contribute most to the observed MOKE data.

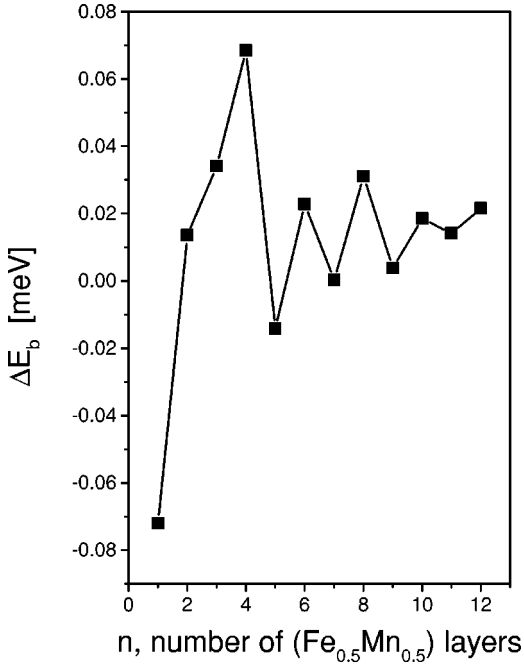

FIG. 14. Band energy part of the magnetic anisotropy energy in $Cu(100)/Cu_6/Co_6/(Fe_{0.5}Mn_{0.5})_n/Vac$ versus n, the number of $(Fe_{0.5}Mn_{0.5})$ layers.

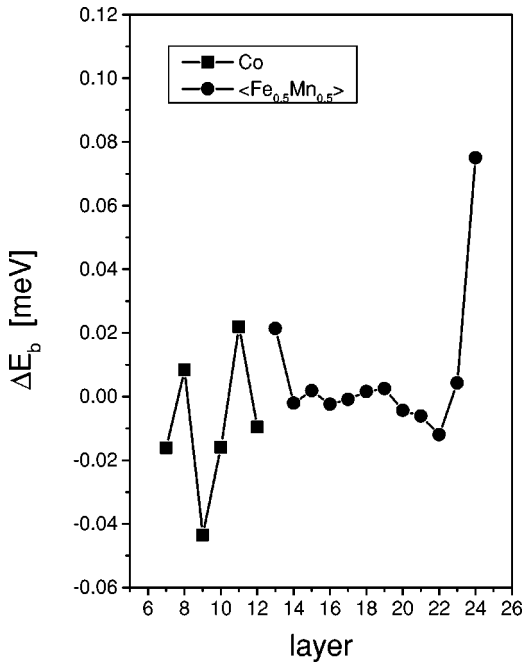

FIG. 15. Layer-resolved band energy part of the magnetic anisotropy energy in $Cu(100)/Cu_6/Co_6/(Fe_{0.5}Mn_{0.5})_{12}/Vac$. Shown are the Co- and the concentration-averaged $(Fe_{0.5}Mn_{0.5})$ contributions.

V. CONCLUSION

Both the experimental investigations and the theoretical calculations show that the system $Cu(100)/Co_m/(Fe_xMn_{1-x})_n$ is indeed very interesting and well suited to be used in terms of spin valves of the type $Cu(100)/Co_p/Cu_s/Co_m/(Fe_xMn_{1-x})_n$/cap with s falling in the regime of antiferromagnetic coupling with respect to the Cu spacer thickness. Such a system provides at room temperature an ''antiferromagnetic'' part, namely, the $(Fe_xMn_{1-x})_n$ slab that not only pins the orientation of the magnetization in the neighboring Co layer, but at the same time acts as a soft ferromagnet. Similar systems with permalloy ($Ni_{80}Fe_{20}$) replacing the Co slabs[14] or using both Co and permally slabs[15] showed a giant magnetoresistance of about 2–5 %, depending on the applied preparation techniques.

In using Cu as cap might open up the possibility to operate such a spin valve also in the current perpendicular to the planes of atoms geometry, since it can be expected that one has to deal with metal like behavior only, i.e., one has to handle only rather small resistivities and thus can circumvent one of the disadvantages of using, for example, oxidic antiferromagnetic parts (large resistances). Further theoretical investigations along this line[12,13] are presently carried out.

It was shown in this paper that the theoretical calculations not only fit very well the available experimental evidence, but also provide a theoretical description that does not rely on classical spin models. Clearly enough, the description applied is based entirely on collinear magnetic configurations: a possible occurrence of noncollinearity has yet to be taken into account.

ACKNOWLEDGMENTS

Financial support was provided partially by the RTN network ''Magnetoelectronics'' (Contract No. HPRN-CT-2000-00143), the Austrian Ministry of Science (Project No. GZ 45.504), the Hungarian National Science Foundation (Contracts Nos. OTKA T030240 and T038162), and by the Research and Technological Cooperation Project between Austria and Hungary (Contract No. A-23/01).

[1] W. Kuch, F. Offi, L.I. Chelaru, M. Kotsugi, K. Fukumoto, and J. Kirschner, Phys. Rev. B **65**, 140408(R) (2002).
[2] F. Offi, W. Kuch, and J. Kirschner, Phys. Rev. B **66**, 064419 (2002).
[3] F. Offi, W. Kuch, L. I. Chelaru, K. Fukumoto, M. Kotsugi, and J. Kirschner, Phys. Rev. B (to be published).
[4] F. Offi, Ph.D. thesis, University of Halle-Wittenberg, 2002.
[5] P. Weinberger and L. Szunyogh, Comput. Mater. Sci. **17**, 414 (2000).
[6] P. Weinberger, P.M. Levy, J. Banhart, L. Szunyogh, and B. Újfalussy, J. Phys.: Condens. Matter **8**, 7677 (1996).
[7] P. Weinberger, Philos. Mag. B **75**, 509 (1997).
[8] S.H. Vosko, L. Wilk, and M. Nusair, Can. J. Phys. **58**, 1200 (1980).
[9] A. Vernes, L. Szunyogh, and P. Weinberger, J. Appl. Phys. **91**, 7191 (2002).
[10] A. Vernes, L. Szunyogh, and P. Weinberger, Phys. Rev. B **65**, 144448 (2002).
[11] A. Vernes, L. Szunyogh, and P. Weinberger, Phys. Rev. B **66**, 214404 (2002).
[12] C. Blaas, L. Szunyogh, P. Weinberger, C. Sommers, P.M. Levy, and J. Shi, Phys. Rev. B **65**, 134427 (2002).
[13] P. Weinberger, L. Szunyogh, C. Blaas, and C. Sommers, Phys. Rev. B **64**, 184429 (2001).
[14] K.-M.H. Lenssen, A.E.M. De Veirman, and J.J.T.M. Donkers, J. Appl. Phys. **81**, 4915 (1997).
[15] L. Tang and D.E. Laughlin, J. Appl. Phys. **81**, 4906 (1997).